J. Phys.: Condens. Matter **24** (2012) 135402 (5pp) doi:10.1088/0953-8984/24/13/135402

Phonon properties of $CoSb_2$ single crystals

N Lazarević[1], M M Radonjić[2], Rongwei Hu[3,4], D Tanasković[2], C Petrovic[3] and Z V Popović[1]

[1] Center for Solid State Physics and New Materials, Institute of Physics Belgrade, University of Belgrade, Pregrevica 118, 11080 Belgrade, Serbia
[2] Scientific Computing Laboratory, Institute of Physics Belgrade, University of Belgrade, Pregrevica 118, 11080 Belgrade, Serbia
[3] Condensed Matter Physics and Materials Science Department, Brookhaven National Laboratory, Upton, NY 11973-5000, USA

Received 28 December 2011, in final form 8 February 2012
Published 9 March 2012
Online at stacks.iop.org/JPhysCM/24/135402

Abstract
The phonon properties of $CoSb_2$ have been investigated by Raman scattering spectroscopy and lattice dynamics calculations. Sixteen out of eighteen Raman active modes predicted by factor-group analysis are experimentally observed and assigned. The calculated and measured phonon energies at the Γ point are in very good agreement. The temperature dependence of the A_g symmetry modes is well represented by phonon–phonon interactions without contribution from any other phonon or electron related interactions.

(Some figures may appear in colour only in the online journal)

1. Introduction

Transition metal dipnictides are of great technological and fundamental importance due to their unusual transport, thermoelectric, and magnetic properties as well as their strength and durability (dinitrides). This class of compounds can have pyrite, marcasite or arsenopyrite type structures [1, 2]. So far, only the phonon properties of marcasite and pyrite type structures have been studied [3–5].

$CoSb_2$ is a semiconductor with arsenopyrite type crystal structure [6, 7]. This compound undergoes a phase transition at 377 °C from the arsenopyrite to marcasite type structure (isostructural to $FeSb_2$) [8, 9]. Recent study of $Fe_{1-x}Co_xSb_2$ ($0 \leq x \leq 1$) alloys [10] revealed a very rich phase diagram that offers the opportunity to study the evolution of conductivity and magnetic ground states in the Kondo-like semiconductor $FeSb_2$ by Co alloying. It is shown that phonons might play an important role in the physical properties of the $Fe_{1-x}Co_xSb_2$ marcasite phase [11, 12]. Since the electronic structure of $CoSb_2$ should be very similar to $FeSb_2$ [2], the investigation of $CoSb_2$ may provide a better understanding of the properties of $FeSb_2$. By alloying with Co, the strong electron–phonon interaction in $FeSb_2$ is significantly reduced [13]. At about $x = 0.5$ this compound undergoes a structural phase transition to the arsenopyrite phase of $CoSb_2$ [10]. Although, $CoSb_2$ is generally accepted as the prototype for a considerable number of binary transition metal pnictides [14, 15], its phonon properties are unknown. In a paper dealing with Raman scattering of the $Fe(Co)Sb_2$ system, unpolarized Raman spectra of $CoSb_2$ were published without any analysis or mode assignment [16].

In this paper, we report polarized Raman scattering spectra measured on differently oriented $CoSb_2$ single-crystal samples at various temperatures. The zone-center optical modes were classified by a factor-group analysis and their energies were obtained using first-principle lattice dynamics calculations. We have obtained very good agreement of our calculated energies with the experimentally observed Raman active modes. We have also analyzed the change of energy by lowering the temperature for the most intense A_g Raman active modes.

2. Experiment

Single crystals of $CoSb_2$ were grown using the high-temperature flux method. Sample structure and composition

[4] Present address: Department of Physics, University of Maryland, College Park, MD 20742-4111, USA.

Table 1. Raman tensors for monoclinic crystal structure and selection rules for the $(1\bar{1}0)$ plane of $CoSb_2$ single crystal together with Raman mode energies (in cm^{-1}) of $CoSb_2$ single crystal.

Raman tensors			Selection rules for the $(1\bar{1}0)$ plane of $CoSb_2$		
$A_g = \begin{pmatrix} a & d & 0 \\ d & b & 0 \\ 0 & 0 & c \end{pmatrix}$		$B_g = \begin{pmatrix} 0 & 0 & e \\ 0 & 0 & f \\ e & f & 0 \end{pmatrix}$	(c, c)	$\longrightarrow$	A_g
			$(\perp c, c)$	$\longrightarrow$	$A_g + B_g$
			$(\perp c, \perp c)$	$\longrightarrow$	$A_g + B_g$

Raman active modes						Infrared active modes			
Symmetry	Exp.	Calculations	Symmetry	Exp.	Calculations	Symmetry	Calculations	Symmetry	Calculations
A_g^1	63.8	68.7	B_g^1	80.9	70.5	A_u^1	99.7	B_u^1	133.3
A_g^2	93.7	97.7	B_g^2	91.1	98.9	A_u^2	108.3	B_u^2	144.2
A_g^3	102.5	104.1	B_g^3	109.7	111.5	A_u^3	142.7	B_u^3	166.6
A_g^4	136.5	141.5	B_g^4	134.4	140.3	A_u^4	167.4	B_u^4	174.4
A_g^5	153.9	154.3	B_g^5	179.6	187.6	A_u^5	174.6	B_u^5	214.6
A_g^6	168.0	171.8	B_g^6	187.3	190.5	A_u^5	205.5	B_u^5	235.9
A_g^7	221.2	220.3	B_g^7	217.6	221.8	A_u^7	224.8	B_u^7	249.4
A_g^8	239.6	238.3	B_g^8		235.5	A_u^8	265.7		
A_g^9	256.6	253.5	B_g^9		252.6				

were determined by analyzing the powder x-ray diffraction data on $CoSb_2$ single crystals collected using a Rigaku Miniflex diffractometer with Cu Kα radiation. The Raman scattering measurements were performed using a Jobin Yvon T64000 Raman system in micro-Raman configuration. The 514.5 nm line of an Ar^+/Kr^+ mixed gas laser was used as the excitation source. Focusing of the laser beam was realized with a long distance microscope objective (magnification 50×). We have found that a laser power level of 0.02 mW on the sample is sufficient to obtain a Raman signal and, except for the signal to noise ratio, no changes of the spectra were observed as a consequence of laser heating by further lowering the laser power. The corresponding excitation power density was less then 0.1 kW cm^{-2}. Low temperature measurements were performed between 80 and 300 K using a KONTI CryoVac cryostat with a 0.5 mm thick window.

3. Results and discussion

$CoSb_2$ crystallizes in the monoclinic structure of the $P2_1/c$ (C_{2h}^5) space group. The unit cell parameters are $a = 0.650\,51(6)$ nm, $b = 0.638\,33(5)$ nm, $c = 0.654\,10(6)$ nm, $\beta = 117.65(1)^\circ$ and $Z = 4$ [9]. All atoms are in (4e) Wyckoff positions [14]. Factor-group analysis yields a normal mode distribution at the center of the Brillouin zone:

$$\Gamma_{CoSb_2} = 9A_g + 9B_g + 9A_u + 9B_u.$$

According to this representation, in the Raman scattering experiment one can expect a total of 18 Raman active modes. We have used the $(1\bar{1}0)$ plane of a $CoSb_2$ single crystal for the Raman scattering measurements. The selection rules for parallel and crossed polarization from the $(1\bar{1}0)$ plane are summarized in table 1. The (c, c) configuration denotes that the polarizer and analyzer polarization direction are parallel to the c axis of the $CoSb_2$ crystal. In this case, only the A_g symmetry modes can be observed. For other parallel $(\perp c, \perp c)$ or crossed $(\perp c, c)$ polarization configurations both the A_g and B_g symmetry modes can be observed.

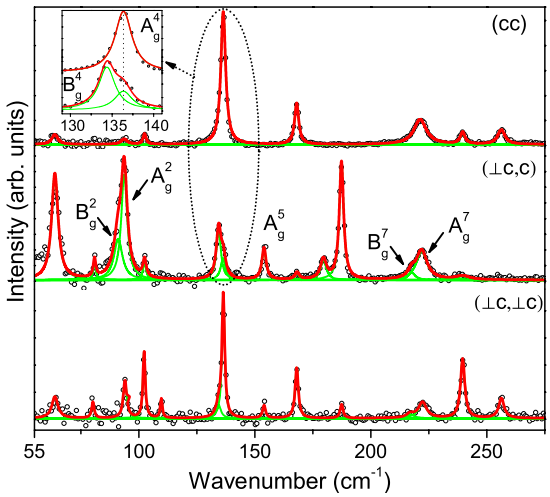

Figure 1. The room-temperature-polarized Raman spectra of $CoSb_2$ single crystals in three polarization configurations. The notation in parentheses indicates the polarization directions of the incident and scattered light, respectively.

The room-temperature-polarized Raman spectra of $CoSb_2$ single crystals in all three polarization configurations are presented in figure 1. The notations are those from table 1. In the (c, c) polarization configuration eight A_g symmetry modes are observed. In both the $(\perp c, c)$ and $(\perp c, \perp c)$ polarization configurations, besides the already observed A_g symmetry modes, five additional peaks were observed. These peaks are assigned according to the selection rules given in table 1, as the B_g symmetry modes. In addition, one can see that in the $(\perp c, c)$ polarization configuration peaks at about 93, 135 and 221 cm^{-1} appear as asymmetric structure. These two peak structures are well fitted with two Lorentzian profile lines, as shown in figure 1. Since higher energy modes of these

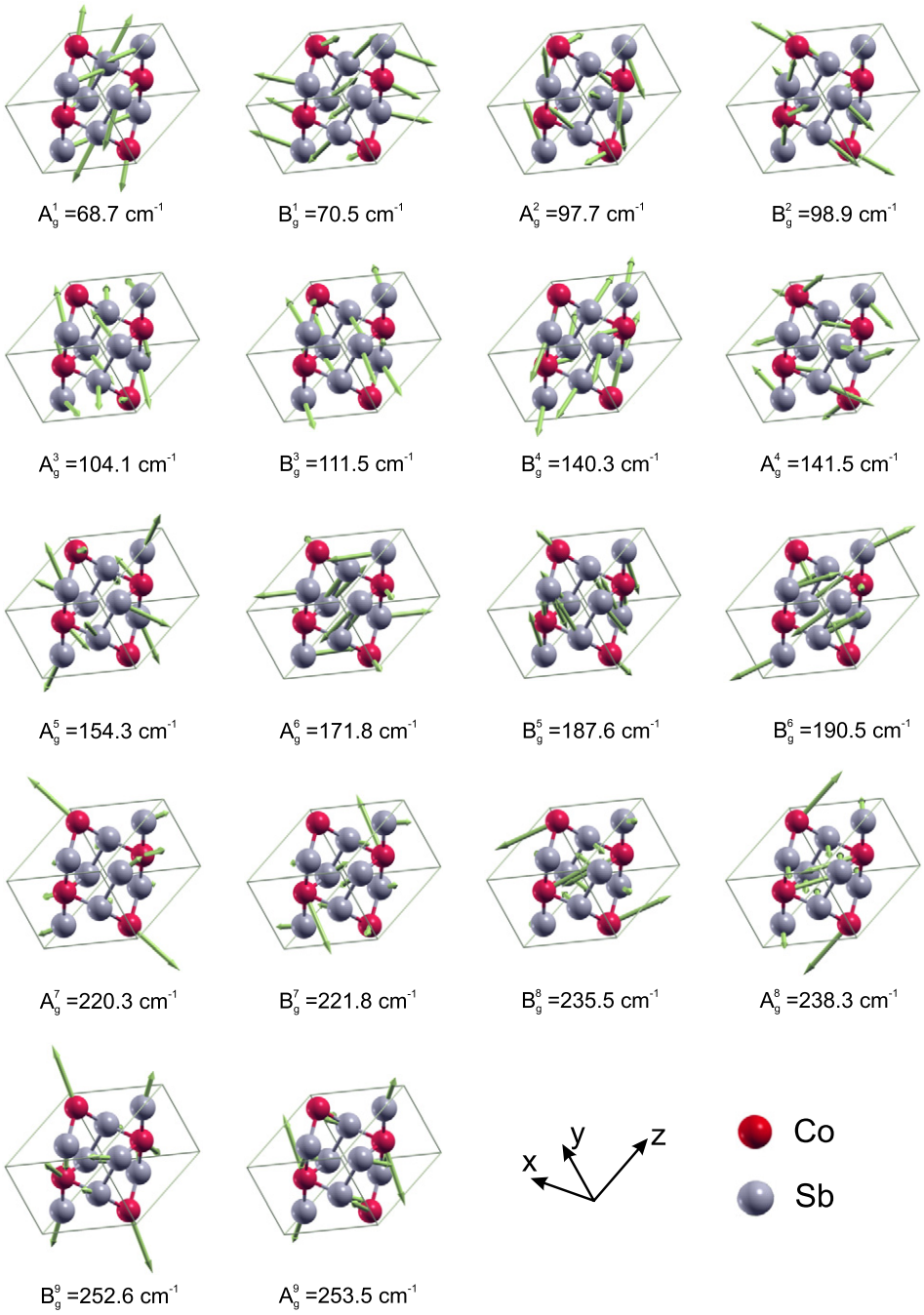

Figure 2. Atomic displacement patterns for the Raman active vibrational modes of $CoSb_2$. The lengths of the arrows are proportional to the square roots of the vibration amplitudes.

doublets have also been observed in the (c, c) configuration (A_g symmetry modes), we have assigned the lower energy modes as the B_g symmetry. Table 1 summarizes $CoSb_2$ Raman mode symmetries and related energies.

The lattice dynamics of $CoSb_2$ was calculated within the framework of density functional perturbation theory (DFPT), as implemented in the QUANTUM ESPRESSO [17] package. We applied the plane-wave basis method with the local density approximation (LDA), with the Perdew–Zunger exchange–correlation functional. This approach was used to calculate the ultra-soft pseudopotentials for cobalt (antimony) taking into account $4s^1 3d^8 4p^0$ ($5s^2 5p^3$) valence electrons. The calculation was performed using the experimentally determined unit cell parameters. The Brillouin zone (BZ) was sampled with an $8 \times 8 \times 8$ Monkhorst–Pack k-space mesh. The calculations start from previously calculated ground state atomic and electronic configurations and continue with self-consistent calculations of the charge response for each different displacement. The calculated normal modes of the Raman active phonons in the center of the BZ (Γ point) are given in figure 2.

On comparing our calculations with the experimental Raman active phonons we found very good agreement. Besides, we assigned the 153.9 cm^{-1} mode as the A_g

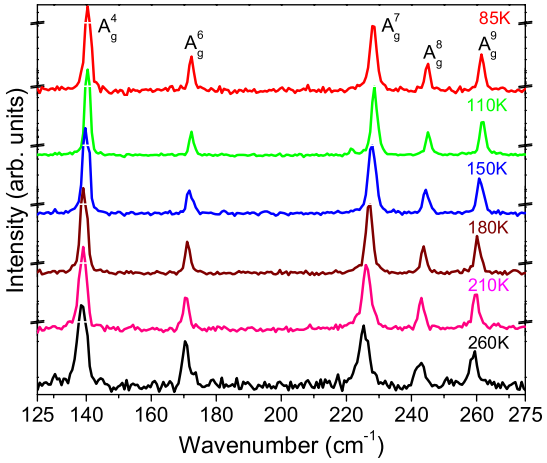

Figure 3. The (c, c) polarized Raman scattering spectra of $CoSb_2$ measured at different temperatures.

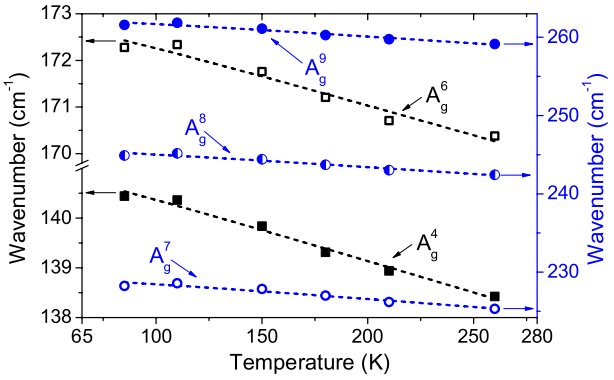

Figure 4. The energies of the highest intensity A_g modes of $CoSb_2$ single crystals as a function of temperature.

symmetry one (A_g^5), although this mode did not appear in the (c, c) polarization, but did in both $(\perp c, c)$ and $(\perp c, \perp c)$ polarizations. Although the calculations were performed at zero temperature and the polarized Raman scattering spectra were obtained at room temperature, we found that all sixteen experimentally observed Raman active modes were in very good agreement with the calculated phonon energies in the Γ point. This is not surprising since the Raman active modes of $CoSb_2$ have a very weak temperature dependence, as will be discussed later. The calculated energies at the Γ point of the infrared active modes are also presented in table 1.

The (c, c) polarized Raman scattering spectra of $CoSb_2$ single crystals (A_g symmetry modes) measured at different temperatures are presented in figure 3. The temperature dependences of the energies of the highest intensity A_g modes of $CoSb_2$ are shown in figure 4. The influence of the anharmonic effects on the Raman mode energy can be taken into account via three-phonon processes [18],

$$\Omega(T) = \Omega_0 - C\left(1 + \frac{2}{e^x - 1}\right), \qquad (1)$$

where Ω_0 is the temperature independent contribution to the Raman mode energy, C is the anharmonic constant and $x = \hbar\Omega_0/2k_BT$. Equation (1) gives a rather good fit (dashed lines in figure 4) of the experimental data, suggesting the absence of any additional temperature dependent couplings (i.e. electron–phonon interaction) in the 80–300 K temperature range. By inspecting the fit parameters presented in table 2, one can see that the temperature dependence of the A_g symmetry mode energy is completely driven by the weak anharmonic effect.

4. Conclusion

By analyzing the Raman scattering spectra for different polarization configurations, sixteen out of eighteen Raman active modes predicted by factor-group analysis have been successfully observed and assigned. The calculated phonon energies at the Γ point are in very good agreement with the experimental data. We find that the temperature dependent energy shift of the highest intensity A_g symmetry modes is well represented by the anharmonic contribution.

Table 2. Best fitting parameters for the energy–temperature dependence of the A_g symmetry mode using equation (1).

Symmetry	Ω_0 (cm^{-1})	C (cm^{-1})
A_g^4	141.76(13)	0.65(3)
A_g^6	173.7(3)	0.82(8)
A_g^7	231.0(5)	1.7(2)
A_g^8	247.3(4)	1.6(2)
A_g^9	264.0(4)	1.7(2)

Acknowledgments

This work was supported by the Serbian Ministry of Education and Science under Projects ON171032, III45018 and ON171017. Part of this work was carried out at the Brookhaven National Laboratory which is operated for the Office of Basic Energy Sciences, US Department of Energy by Brookhaven Science Associates (DE-Ac02-98CH10886) (RH and CP). Numerical simulations were run on the AEGIS e-Infrastructure, supported in part by FP7 projects EGI-InSPIRE, PRACE-1IP and HP-SEE. ZVP and MMR acknowledge support from the Swiss National Science Foundation through the SCOPES Grant No. IZ73Z0-128169.

References

[1] Kjekshus A and Brostigen G 1970 *Acta Chem. Scand.* **24** 2983–92
[2] Goodenough J B 1972 *J. Solid State Chem.* **5** 144–52
[3] Lutz H D and Müller B 1991 *Phys. Chem. Miner.* **17** 716–9
[4] Lutz H D and Müller B 1991 *Phys. Chem. Miner.* **18** 265–8
[5] Lazarevic N, Radonjic M M, Tanaskovic D, Hu R, Petrovic C and Popovic Z V 2011 arXiv:1108.0581v1
[6] Rosenqvist T 1953 *Acta Metall.* **1** 761–3
[7] Hulliger F 1963 *Phys. Lett.* **4** 282–3
[8] Kjekshus A and Rakke T 1977 *Acta Chem. Scand.* **31** 517–29
[9] Siegrist T and Hulliger F 1986 *J. Solid State Chem.* **63** 23

[10] Hu R, Mitrović V F and Petrovic C 2006 *Phys. Rev.* B **74** 195130
[11] Tomczak J M, Haule K, Miyake T, Georges A and Kotliar G 2010 *Phys. Rev.* B **82** 085104
[12] Diakhate M S, Hermann R P, Möchel A, Sergueev I, Søndergaard M, Christensen M and Verstraete M J 2011 *Phys. Rev.* B **84** 125210
[13] Lazarević N, Popović Z V, Hu R and Petrovic C 2010 *Phys. Rev.* B **81** 144302
[14] Kjekshus A 1971 *Acta Chem. Scand.* **25** 411–22
[15] Chen W, Tse J S and Jiang J Z 2010 *Solid State Commun.* **150** 181–6
[16] Lazarević N, Popović Z V, Hu R and Petrovic C 2009 *Phys. Rev.* B **80** 014302
[17] Giannozzi P *et al* 2009 *J. Phys.: Condens. Matter* **21** 395502
[18] Balkanski M, Wallis R F and Haro E 1983 *Phys. Rev.* B **28** 1928–34